Stabilising Barrel Transportation by Modelling Inverted Pendulums

Jacob Downs, Jack Foster-Ogg, Mike Nelhams, Elfa Ren GROUP 5

uf18184@bristol.ac.uk, mm18034@bristol.ac.uk, oa18502@bristol.ac.uk, uk18700@bristol.ac.uk

November 6, 2020

Abstract

Equations of motion and control theory for stabilisation of a pendulum in the vertical position are reasonable approaches for stabilising barrel transportation. We aim to model a cart-barrel system which is moving horizontally by proposing a control law to stabilise the pendulum in the vertical position under cart moving conditions. In this paper, we first proposed a model with its equations of motion, to simulate the movement of an inverted pendulum on a cart. Next, we converted the equations into a state-space representation and we found a way to test the stability of the system. We finally created a closed-loop control system on MATLAB including the use of a linear quadratic regulator. The proposed simulation and state-space of equations accurately replicate the complexity of the actual mechanical system, however, in linearising the initial system of equations, some precision was lost. The state-space solution can only stabilise the barrel if the barrel begins within a rotation of 20° from the vertical. Consequently, if there is an unforeseen accident to the cart then the barrel will be unrecoverable beyond the 20° limits. In this paper, further advancements are suggested through the use of artificial intelligence techniques such as reinforcement learning and fuzzy logic and this could greatly reduce the time to stabilise the barrels and extend the range of angles through which the barrels may rotate.

1 Introduction of Contextualised Stability Principles

Stability is a key engineering concept when controlling systems, requiring modelling of differential equations with one or more arbitrary functions subjected to restrictions [1]. Stability is also paramount in nature, with the environmental function of homeostasis in metabolism and the development of living cells having proposed negative feedback loops, to provide stability [2]. From the core principles of stability

$$\frac{dU}{d\theta} = 0, \tag{1}$$

at positions of equilibrium. With U being the total potential energy of the conservative system and θ the angle of rotation of the inverted pendulum [3]. There may be several points of equilibrium in a system depending on the order of U. A position is stable if the system will move back to the equilibrium state after being slightly displaced. This can be verified mathematically, if

$$\frac{d^2U}{d\theta^2} > 0, \tag{2}$$

then the system is in stable equilibrium for the respective equilibrium θ value. Contrasting a position is unstable if the system will move away from its initial state after a small displacement, given by the comparative

$$\frac{d^2U}{d\theta^2} < 0. \tag{3}$$

Intuitively an inverted pendulum has two obvious points of equilibrium, one at the top of its arc and one at the bottom where it will hang. Applying this to the context of our problem we can see the different states in figure 1.

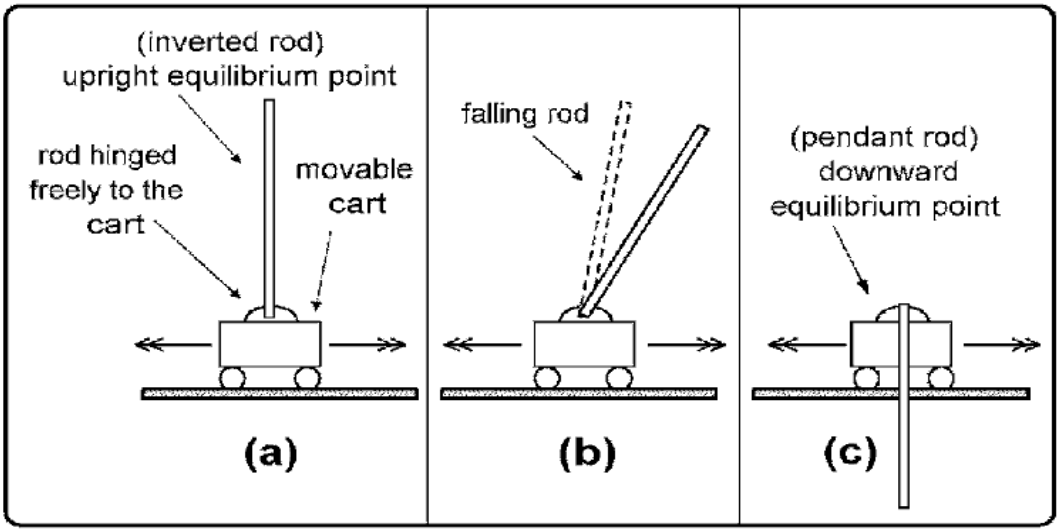

Figure 1: *Illustration of equilibrium states for an inverted pendulum mounted on a cart [4].*

Without having to do any calculations we can presume the position at the top is unstable by intuition, (a) in figure 1. A small displacement to this position will force the pendulum to fall down to the stable state, (c). We will focus on the unstable equilibrium of this system, trying to control the pendulum at this state, managing any displacements appropriately.

We can analyse the behaviour of a system's stability by changing the parameters of the model to find the optimal solution to maximise an objective. Our model's objective is to keep the inverted rod vertically upright during its motion. A model is considered unstable if it does not return to its initial position but instead continues to oscillate after it is subjected to any change in input [5].

Using a Newtonian method we can formulate the equations of motions for the non-linear inverted pendulum motion whilst mounted on a moving cart with the given typical parameters first. We can then create a control system and once we are happy with the performance at the standard values we can execute robust testing. Robust control aims to design a fixed controller such that a level of performance is guaranteed, irrespective of changes in the dynamics of the system within a predefined boundary [6]. Running our model with irregular, initial angular displacements, we can see from the simulations whether the system can stabilise despite the uncertain starting parameters.

Inverted pendulum systems appear frequently in nature, from simply balancing a broomstick to the human body's nervous system which uses a feedback process to keep our bodies upright. The vertical posture of a human body can be modelled as a single inverted pendulum rotating around a pin joint, the ankle. The joint rotates due to a combination of torques: a passive torque representing the joints viscoelasticity, modelled as a linear spring; an active torque being the reaction of the nervous system modelled by a feedback controller with a time delay. The noise torque refers to the frictional forces in the joint dissipating motor noise. This forms a delay-differential equation (DDE) [7]. This DDE uses inertia principles of the pendulum rotating round the ankle, likewise we will have to include the inertia of the barrels in our Newtonian model. This natural human model can be used to further our understanding on feedback stabilising strategies, adapting and applying this to our problem of minimising barrel oscillations.

Similarly inverted pendulums have been used time and time again in industry [8], with the early designs of seismometers using inverted pendulums as shown in figure 2. The inherent instability property of the inverted pendulum is ideal for reacting to the slightest movements made by small earthquakes [9]. This relates to the delicate process of transporting barrels, with accidents becoming very possible without a rigorous testing process (test-beds).

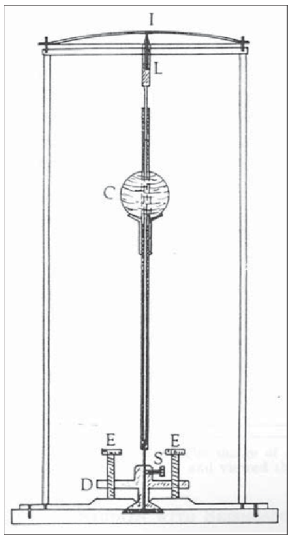

Figure 2: *Seismometer designed by James Forbes in 1844 using an inverted pendulum, S being the pivot [10].*

Other applications of the inverted pendulum include space rocket take-offs, requiring a continuous correction mechanism to keep the rocket upright. Good control is paramount during the extremely unstable launching process [11]. Modelling must be rigorous and robust, with drastic consequences possible. NASA implement a flexible inverted pendulum system to their rockets. This copes with the different compartments of the rocket moving during launch, which can effect overall trajectory [12].

The following report highlights a principle model for maintaining the stability of inverted pendulums Subsequently this report has many industrial applications for transporting barrels and similar fragile goods. All of the simulation code is available from the following GitHub repository: `https://github.com/MikeMNelhams/Mike-Nelhams`.

2 Notation

For the notation in this report:

- M is the mass of the cart (kg)
- m is the mass of the barrel (kg)
- l is the length from the pivot to the centre of mass of the barrel (m)
- g is the gravitational constant 9.81... (ms^{-2})
- I is the moment of inertia of the barrel around the pivot (kgm^2)
- b is the drag constant for the cart (kgs^{-1})
- F is the external force being applied to the cart $(kgms^2)$
- N is the vertical reaction force between the cart and the pendulum $(kgms^2)$
- R is the horizontal reaction force between the cart and the pendulum $(kgms^2)$
- x is the horizontal displacement of the cart (m)
- $\dot{x}$ denotes the first derivative of x
- $\ddot{x}$ denotes the second derivative of x

3 Control Theory State-Space System

3.1 Initial Assumptions

For this model, the following assumptions always hold:

- The barrel is modelled as a uniform rod of length $2l$ (m) and mass m (kg), since barrels are cylindrical.
- The angle of the barrel to the vertical (θ) is always less than 20°, i.e. $|\theta| \leq 20$ and begins vertically at angle of 0°. This assumes the barrels are always loaded upright.
- The rolling resistance between the wheels and the ground is negligible.

3.2 System Analysis

We will be modelling the problem as a cart-pendulum system, with two degrees of freedom: the horizontal position of the cart (x) and the angle of the pendulum to the vertical (θ). Our approach has been based in part on the MATLAB control theory model for an inverted pendulum system: [13]

The system will be controlled by an input force F and we will assume that there are no internal resistances. In this initial model we will also assume the system is only subject to one source of external resistance, drag. As such we are assuming negligible rolling resistance between the cart and the surface it's moving on. We are assuming this drag is a form of Stoke's drag [14], and as such is proportional to the cart's velocity. In reality, Stoke's drag only accurately describes objects with very low Reynold's numbers and therefore this approximation would only be truly accurate when the cart was moving at close to zero speed. However, as we lack more information about the aerodynamics of the cart, Stoke's drag is as reasonable an approximation as we are likely to achieve.

Figure 3 shows a free body diagram representing our system.

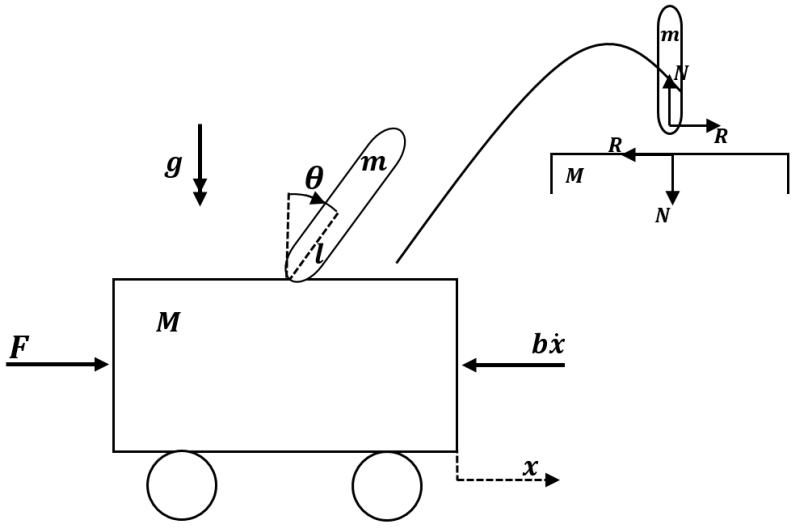

Figure 3: *Force Diagram of the system*

The system is described with parameters in general terms M, m, l and b. We will later substitute these for the problem specific parameters:

$$M = 30\ (kg)$$
$$m = 10\ (kg)$$
$$l = 0.25\ (m)$$
$$b = 0.1\ (kgs^{-2}).$$

In order to better understand the system, the first step was to derive equations of motion to represent it. In order to do this, we first equated the horizontal forces on the cart to give us the following equation (4):

$$F = M\ddot{x} + R + b\dot{x}. \tag{4}$$

Equating the horizontal forces on the pendulum then gave us equation 5:

$$R = m\ddot{x} + ml\dot{\theta}^2 \sin\theta - ml\ddot{\theta}\cos\theta. \tag{5}$$

By substituting equation 5 into equation 4 we got the following equation of motion (6):

$$F = (M+m)\ddot{x} + ml\dot{\theta}^2 \sin\theta - ml\ddot{\theta}\cos\theta + b\dot{x}. \tag{6}$$

We then equated the forces perpendicular to the pendulum to get our fourth equation (7):

$$R\cos\theta - N\sin\theta + mg\sin\theta = ml\ddot{\theta} - m\ddot{x}\cos\theta. \tag{7}$$

In order to eliminate R and N, we then took moments around the centre of the pendulum. This gave us equation 8:

$$Nl\sin\theta = I\ddot{\theta} + Rl\cos\theta. \tag{8}$$

By substituting equation 8 into equation 7 we derived our second equation of motion (equation 9):

$$-I\ddot{\theta} + mgl\sin\theta = ml^2\ddot{\theta} - ml\ddot{x}\cos\theta. \tag{9}$$

As our goal was to minimise the oscillations of the pendulum, we assumed that the angle θ would always be relatively small ($< 0.5rad$). We could therefore use the small angle approximations of $\sin\theta$ and $\cos\theta$, as well as a zero approximation of the expression $\dot{\theta}^2$, to linearise our equations of motion.

$$\sin\theta \approx \theta,\ \cos\theta \approx 1, \dot{\theta}^2 \approx 0. \tag{10}$$

Substituting these approximations into our original equations of motion (6 and 9) gave us the linearised equations of motion (11 and 12):

$$F = (M+m)\ddot{x} - ml\ddot{\theta} + b\dot{x}, \tag{11}$$
$$ml\ddot{x} = (I + ml^2)\ddot{\theta} - mgl\theta. \tag{12}$$

Now that we had our linearised equations of motion we were able to rewrite them as a series of first order differential equations (13, 14, 15 and 16):

$$\dot{x} = \dot{x}, \tag{13}$$

$$\ddot{x} = \frac{-(I+ml^2)b\dot{x} + m^2gl^2\theta + (I+ml^2)F}{(M+m)I + Mml^2}, \tag{14}$$

$$\dot{\theta} = \dot{\theta}, \tag{15}$$

$$\ddot{\theta} = \frac{-mlb\dot{x} + (M+m)mgl\theta + mlF}{(M+m)I + Mml^2}. \tag{16}$$

Having written the equations of motion as first order differentials meant that it was then easy to convert them into a state-space representation. A state-space representation is a powerful tool in systems analysis, allowing straightforward testing of stability, controllability, observability and open-loop response. Our system is best described as a continuous time-invariant state-space of the form:

$$\begin{aligned} \dot{\mathbf{x}} &= A\mathbf{x} + B\mathbf{u} \\ \mathbf{y} &= C\mathbf{x} + D\mathbf{u}. \end{aligned} \tag{17}$$

Where $\mathbf{A}$ is the state matrix which represents the 4 system parameters. Matrix $\mathbf{B}$ is the input matrix, which represents the force applied to the system. Matrix $\mathbf{C}$ is the output matrix which represents the observable outputs, x and θ. Matrix $\mathbf{D}$ is the 'feed-through' matrix, however, since this model has direct feedback, therefore $\mathbf{D} = \mathbf{0}$. The input force F has been substituted for u for the remainder of the derivation. Our system is a one-input, two-output state-space control system.

Converting our first order differential equations into a state-space of this form gave us the following (18 and 19):

$$\begin{bmatrix} \dot{x} \\ \ddot{x} \\ \dot{\theta} \\ \ddot{\theta} \end{bmatrix} = \begin{bmatrix} 0 & 1 & 0 & 0 \\ 0 & \frac{-(I+ml^2)b}{(M+m)I+Mml^2} & \frac{m^2gl^2}{(M+m)I+Mml^2} & 0 \\ 0 & 0 & 0 & 1 \\ 0 & \frac{-mlb}{(M+m)I+Mml^2} & \frac{(M+m)mgl}{(M+m)I+Mml^2} & 0 \end{bmatrix} \begin{bmatrix} x \\ \dot{x} \\ \theta \\ \dot{\theta} \end{bmatrix} + \begin{bmatrix} 0 \\ \frac{I+ml^2}{(M+m)I+Mml^2} \\ 0 \\ \frac{ml}{(M+m)I+Mml^2} \end{bmatrix} u, \tag{18}$$

$$\mathbf{y} = \begin{bmatrix} 1 & 0 & 0 & 0 \\ 0 & 0 & 1 & 0 \end{bmatrix} \begin{bmatrix} x \\ \dot{x} \\ \theta \\ \dot{\theta} \end{bmatrix} + \begin{bmatrix} 0 \\ 0 \end{bmatrix} u. \tag{19}$$

Substituting the model specific parameters into this state-space then gave us the following (20 and 21):

$$\begin{bmatrix} \dot{x} \\ \ddot{x} \\ \dot{\theta} \\ \ddot{\theta} \end{bmatrix} = \begin{bmatrix} 0 & 1 & 0 & 0 \\ 0 & -0.003077 & 2.262 & 0 \\ 0 & 0 & 0 & 1 \\ 0 & -0.009231 & 36.18 & 0 \end{bmatrix} \begin{bmatrix} x \\ \dot{x} \\ \theta \\ \dot{\theta} \end{bmatrix} + \begin{bmatrix} 0 \\ 0.03077 \\ 0 \\ 0.09231 \end{bmatrix} u, \tag{20}$$

$$\mathbf{y} = \begin{bmatrix} 1 & 0 & 0 & 0 \\ 0 & 0 & 1 & 0 \end{bmatrix} \begin{bmatrix} x \\ \dot{x} \\ \theta \\ \dot{\theta} \end{bmatrix} + \begin{bmatrix} 0 \\ 0 \end{bmatrix} u. \tag{21}$$

Having represented the pendulum and cart in this way, we could then test the stability of the system. In order to do this we had to find the system poles by taking the eigenvalues of matrix $\mathbf{A}$.

$$Poles \;=\; 0,\; -0.0025,\; -6.0157,\; 6.0151. \tag{22}$$

The existence of a positive real pole (6.0151) told us that the system was unstable, which had been expected. We then tested the open-loop step response of the system, with a one Newton step, over a time period of 5 seconds. The result is represented in figure 4.

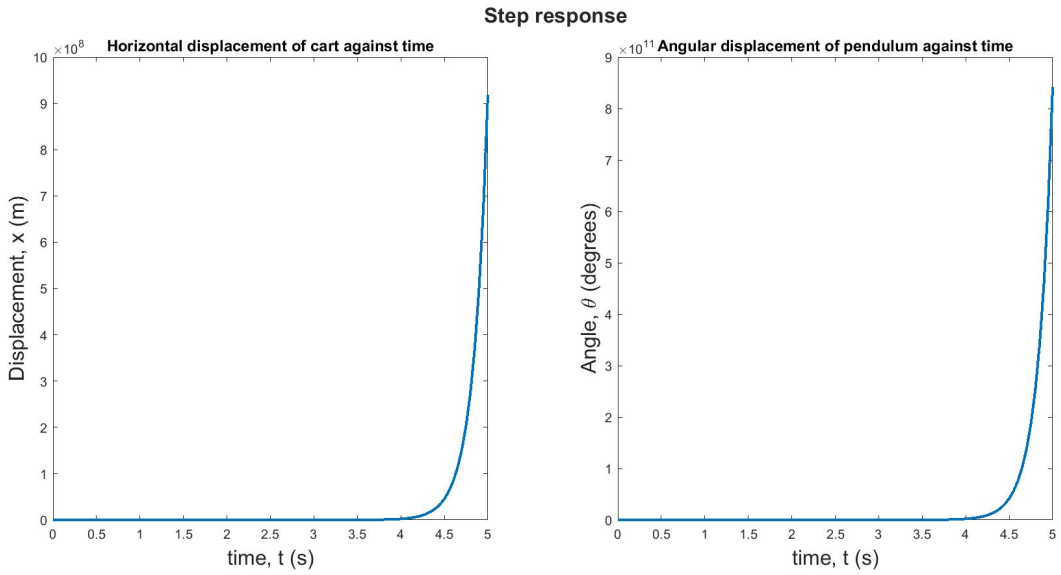

Figure 4: *Open-loop step response of system, with a ten Newton step and time period of 5 seconds. Shows that the system is very unstable in an open-loop.*

Figure 4 shows the pendulum angle spike to an extreme $9 \cdot 10^{11}$ degrees in just 5 seconds. This is in part a result of our reliance on small angle trigonometric approximations, causing an exponential increase in both the x and θ outputs. However, it also represented the underlying instability of the system and showed that, in order to meet our objective of minimising pendulum oscillations, we would have to create a robust input control. To do this, however, we would first have to ascertain whether or not the system was controllable. We did this by creating a controllability matrix [15] and then assessing its rank:

$$\text{Controllability Matrix} = \begin{bmatrix} \mathbf{B} & \mathbf{AB} & \mathbf{A^2B} & \mathbf{A^3B} \end{bmatrix} \tag{23}$$

$$= \begin{bmatrix} 0 & 0.0308 & -0.0001 & 0.2088 \\ 0.0308 & -0.0001 & 0.2088 & -0.0013 \\ 0 & 0.0923 & -0.0003 & 3.3401 \\ 0.0923 & -0.0003 & 3.3401 & -0.0122 \end{bmatrix} \tag{24}$$

The controllability matrix has dimensions 4 by 4 and rank 4 (full rank), so the system is controllable. In order to create a robust closed-loop control system, it is also useful to assess the observability of the system. We did this in a similar fashion, creating an observability matrix and assessing its corresponding rank.

$$\text{Observability Matrix} = \begin{bmatrix} \mathbf{C} \\ \mathbf{CA} \\ \mathbf{CA^2} \\ \mathbf{CA^3} \end{bmatrix} \tag{25}$$

$$= \begin{bmatrix} 1.0000 & 0 & 0 & 0 \\ 0 & 0 & 1.0000 & 0 \\ 0 & 1.0000 & 0 & 0 \\ 0 & 0 & 0 & 1.0000 \\ 0 & -0.0031 & 2.2615 & 0 \\ 0 & -0.0092 & 36.1846 & 0 \\ 0 & 0.0000 & -0.0070 & 2.2615 \\ 0 & 0.0000 & -0.0209 & 36.1846 \end{bmatrix} \tag{26}$$

The observability matrix was also full rank, with dimensions 8 by 4 and rank 4, so the system is both controllable and observable. This means a closed feedback loop can be formed with only knowledge of the cart's position x and angle θ.

3.3 Control System

Having analysed the model and built a state-space to describe it, we then attempted to create a control system for it. We initially did this by using a linear quadratic regulator (LQR). The LQR works by minimising the quadratic cost function $\mathbf{J(u)}$ for a system of form $\dot{x} = \mathbf{A}x + \mathbf{B}u$. The LQR then outputs an 'optimal gain vector' K with $u = -Kx$.

$$\mathbf{J(u)} = \int_{\infty}^{0} (x^T \mathbf{Q} x + u^T \mathbf{R} u)\, dt.$$

The parameter $\mathbf{Q}$ is the state-cost weighted matrix and the parameter $\mathbf{R}$ is the input-cost weighted matrix. We initially used Bryson's rule [16] to set the values for $\mathbf{Q}$ and $\mathbf{R}$; these were:

$$\mathbf{Q_0} = \mathbf{C'C} \tag{27}$$

$$= \begin{bmatrix} 1 & 0 & 0 & 0 \\ 0 & 0 & 0 & 0 \\ 0 & 0 & 1 & 0 \\ 0 & 0 & 0 & 0 \end{bmatrix}, \tag{28}$$

$$\mathbf{R} = 1. \tag{29}$$

We then used the optimal gain vector, K, to create a new state-space, with $\mathbf{A} = \mathbf{A} - \mathbf{B}K$:

$$\begin{bmatrix} \dot{x} \\ \ddot{x} \\ \dot{\theta} \\ \ddot{\theta} \end{bmatrix} = \begin{bmatrix} 0 & 1 & 0 & 0 \\ 0.03077 & 0.2855 & -22.78 & -4.18 \\ 0 & 0 & 0 & 1 \\ 0.09231 & 0.8564 & -38.93 & -12.54 \end{bmatrix} \begin{bmatrix} x \\ \dot{x} \\ \theta \\ \dot{\theta} \end{bmatrix} + \begin{bmatrix} 0 \\ 0.03077 \\ 0 \\ 0.09231 \end{bmatrix} u, \tag{30}$$

$$\mathbf{y} = \begin{bmatrix} 1 & 0 & 0 & 0 \\ 0 & 0 & 1 & 0 \end{bmatrix} \begin{bmatrix} x \\ \dot{x} \\ \theta \\ \dot{\theta} \end{bmatrix} + \begin{bmatrix} 0 \\ 0 \end{bmatrix} u. \tag{31}$$

By running the new state-space system with input u equal to the desired cart displacement x, we could simulate the controlled response. Figure 5 shows this simulation run with a displacement objective of 50 metres in the positive x-direction. What we can see is that the control system has been successful, with the cart settling at $x = 50$ and $\theta = 0$ in a time period of less than 60 seconds. We can also see is that the maximum pendulum displacement, θ , is approximately 6°. This is well within our limitation value of 20°, however, it is still a fairly significant deviation from the initial vertical position.

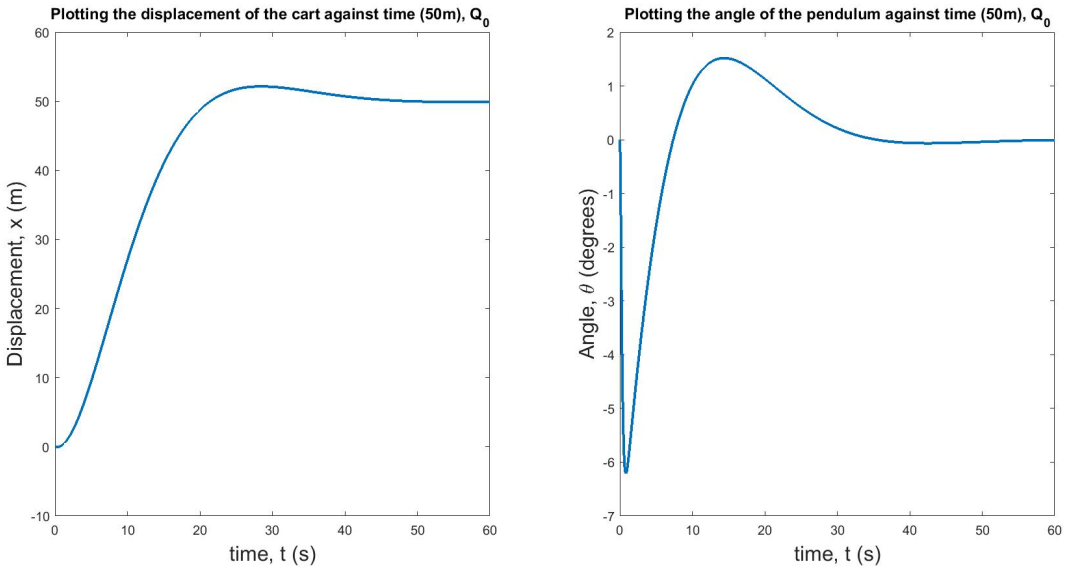

Figure 5: *Closed-loop response for the system with LQR*

3.4 Optimising the Control System

It is possible to optimise the LQR control system by changing the values of the matrix $\mathbf{Q}$. Reducing the value of $Q(1,1)$ should lower the maximum pendulum angle, θ, but increase the systems settling time, t. Increasing the value of $Q(1,1)$ should have the inverse effect, shortening settling time, but increasing the maximum value of θ. This is shown in figures 6 and 7, with figure 6 corresponding to matrix $\mathbf{Q_1}$ and figure 7 corresponding to matrix $\mathbf{Q_2}$.

$$\mathbf{Q_1} = \begin{bmatrix} 0.25 & 0 & 0 & 0 \\ 0 & 0 & 0 & 0 \\ 0 & 0 & 1 & 0 \\ 0 & 0 & 0 & 0 \end{bmatrix}, \tag{32}$$

$$\mathbf{Q_2} = \begin{bmatrix} 4 & 0 & 0 & 0 \\ 0 & 0 & 0 & 0 \\ 0 & 0 & 1 & 0 \\ 0 & 0 & 0 & 0 \end{bmatrix}. \tag{33}$$

What we see is that $\mathbf{Q_1}$ produces a smaller angular deviation of just over 3°, but a large settling time of close to 90 seconds. On the other hand $\mathbf{Q_2}$ produces a settling time of only about 45 seconds, but a maximum angular deviation of almost 12°.

Which $\mathbf{Q}$ Matrix is better to use depends on what the objective of the control system is. If the goal is to move the cart a certain distance as quickly as possible, with more of a focus on the angle the pendulum settles at than its maximum deviation, a larger $Q(1,1)$ value would be better. If, however, the goal is to keep the pendulum angle to a minimum at all times, a smaller $Q(1,1)$ value would be preferred. In the case of our cart stabilisation problem, the latter is likely to be a more relevant goal. Often finding the optimal $\mathbf{Q}$ value comes down to a process of trial and error, balancing desired settling time with maximum angular deviation, to produce the best problem-specific solution.

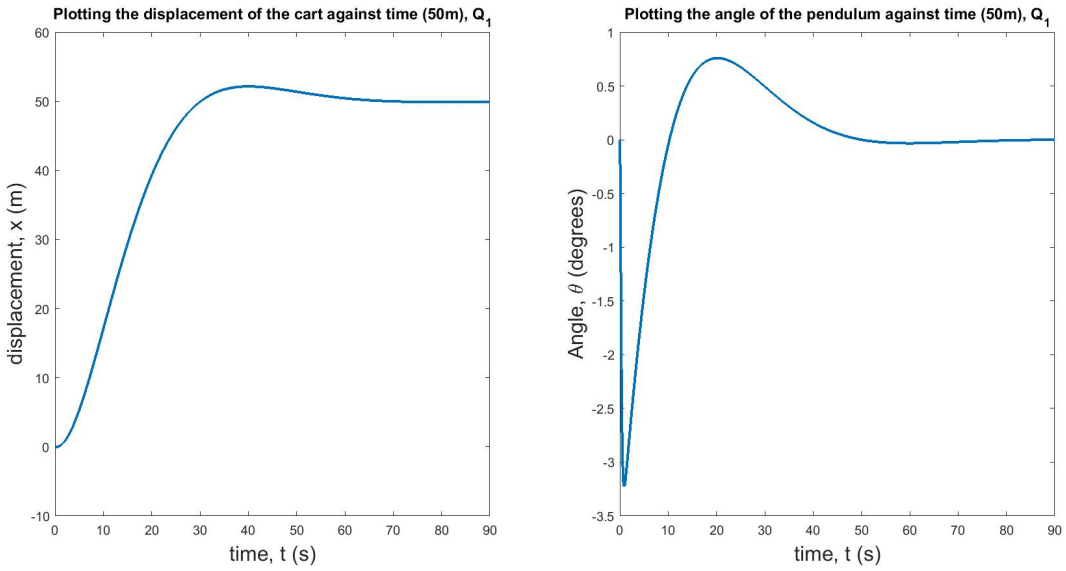

Figure 6: *Closed-loop response for the system with LQR. Optimised for minimal angular deviation by use of small $Q(1,1)$ value. This results in greater settling time as compared to Figure 5 and 7.*

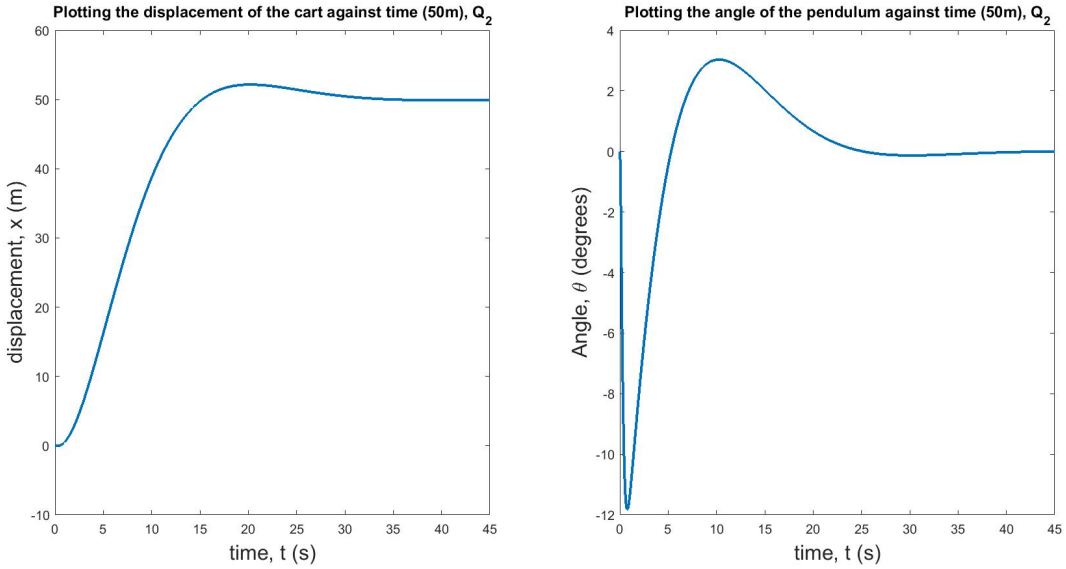

Figure 7: *Closed-loop response for the system with LQR. Optimised for minimal settling time. This results in greater angular deviation as compared to Figure 5 and 6.*

A typical problem that would be expected for this system would be to travel roughly 100m in roughly 20 seconds. By using this model to simulate the barrel and cart system, the two following graphs are shown in figure 9(a). The time limit of 20 seconds is reasonable, but is quite constrained and this limit makes the angle change sharply, peaking to a maximum of 12°. Despite this sharp change, the cart successfully reaches the target distance within the target time as well as the angle being relatively close to 0°. This is an ideal scenario and demonstrates the ability of the model well. If the time was not constrained, then the barrel will limit to 0° (figure 9(b)) within 5 decimal places - a result which is more than adequate.

Figure 8: *The system travelling under expected constraints*

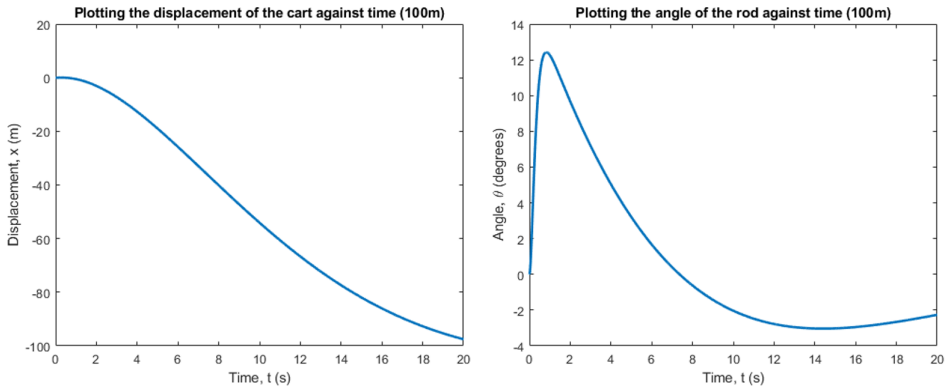

(a) Plotting displacement and angle of the system over time for 100m

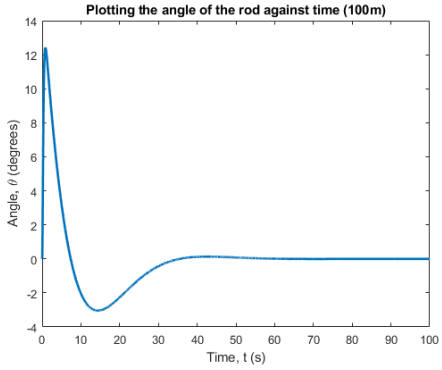

(b) Plotting displacement and angle of the system over time for 100m over 100 seconds

3.5 Further control system developments

Having successfully used the LQR control system over x displacements of both 50 and 100 metres, we then attempted to test the system over longer distances. What we found was that, because the shape of the control system's input remains similar over all distances, increasing the distance objective always results in an increase of maximum angular deviation. It is possible to account for this by further reducing the value $Q(1,1)$ with each increase in the displacement objective x. However, this has a disproportionate effect on settling times and means the control system struggles to scale up easily.

To solve this we came up with a new implementation of the Linear Quadratic Regulator system. On early tests we found that our original LQR system resulted in the majority of the x distance being covered quickly, with most of the allotted time being used to the settle the system. Our new control used this fact to its advantage. By subdividing the objective x distance into a series of smaller distances and running the LQR against these, we were able to produce a scalable control system optimised for both minimal time and minimal angular deviation. This worked by running our initial LQR control system against each new x objective, one after another, on a loop. Because the system is being controlled throughout, it was not necessary to allot it settling time after each loop, instead only allowing it to settle after it had met its final x objective. The advantage of this is that a low $Q(1,1)$ value could be used for each loop, meaning that angular deviation could be minimised. The system could then be forced to settle by running the LQR with a high $Q(1,1)$ value at the end (when the deviation from the final objective was small and so the input required was minimal). You can see the result of this by comparing Figures 9 and 10.

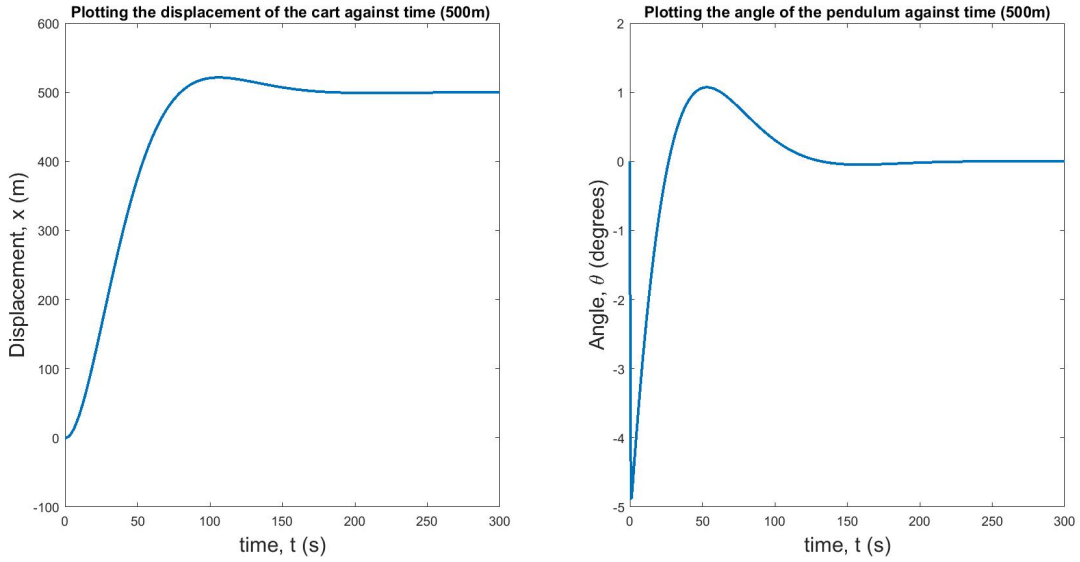

Figure 9: *Response for the system with single closed loop LQR. Run over an x objective of 500m and optimised for minimal angular deviation over a settling time of 300 seconds.*

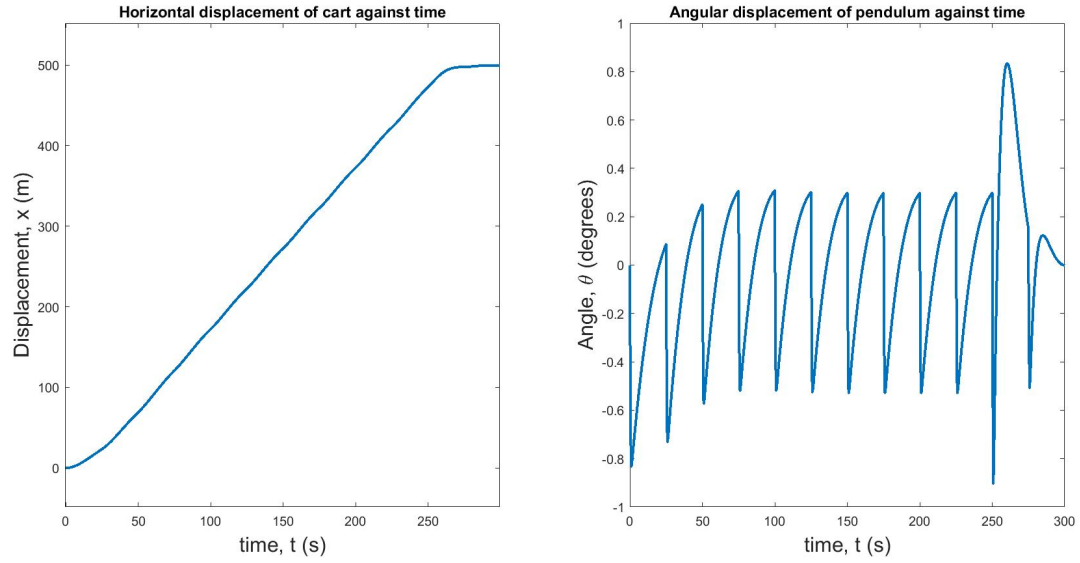

Figure 10: *Response for the system with looped LQR controller. Run over an x objective of 500m and with an allotted settling time of 300 seconds. Displays much smaller angular deviation than the single loop LQR system shown in Figure 9*

Figure 9 shows our best attempt at controlling the system over a distance of 500m, with the standard LQR. What you see is that, even with a settling time of 300 seconds, the angular deviation was still up to 5°. In comparison, when the looped LQR was run with the same distance objective and allotted time, the angular deviation was kept to a comparatively minimal +-1°. Although testing shows both systems to be successful, the looped LQR has the advantage of being easier to optimise for minimal angular deviation and, as such, more scalable over longer distances.

4 Discussion

4.1 Strengths and Limitations

Our models for the cart and inverted pendulum system accurately describe the motion and appropriate stabilisation to keep the pendulum upright. The model is highly accurate for systems in which the rod is given sufficient time to reach its distance. For the case of industrially transporting barrels over long distances, the model should sufficiently keep the barrels upright provided that there is a sufficiently large period of time e.g. 30 seconds to travel. This is a key strength, because the simulation will minimise the force below an acceptable limit, which will increase the time duration of travel (t). The force is kept below a maximum limit, because the cart will run on an engine, which will be limited to a maximum power. Since force is related to power by the given equation:

$$P = \frac{Fx}{t},$$

because the distance (x) and power (P) are constant, then:

$$F \propto t.$$

Consequently, the time duration (t) must increase so as to increase the force (F).

An important limitation to the system is the fact that, due to the small angle approximation, the system cannot re-stabilise the pendulum if the angle (θ) exceeds about 20° in either direction. This is due to the small angle approximation being used to linearise the system of ODE equations (14) and (15) and the way in which the inaccuracy increases past 20° as seen in figure 11. This is a major limitation because if there is an unforeseen circumstance such as an abrupt stop or the barrel rolling, then the barrel will topple completely and the contained delicate materials will be damaged. This would be a considerable downside because if accidents in transportation are expected to be frequent, then the barrels would topple frequently, since the system is not adaptable for sudden changes.

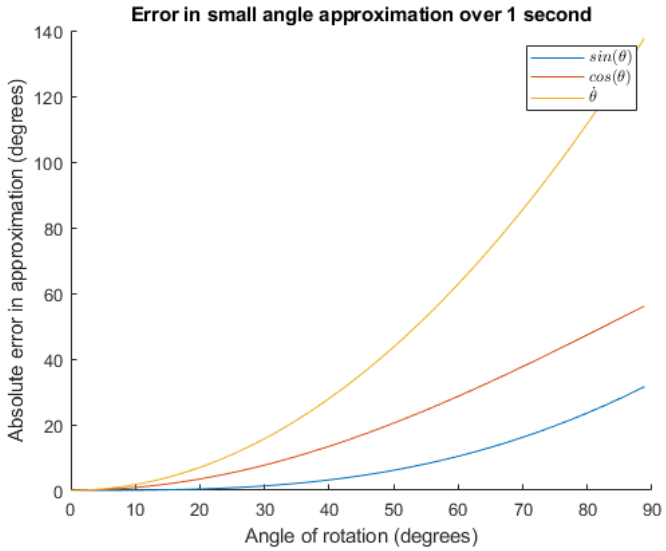

Figure 11: *Error calculation for small angle approximations*

As well as this, it is also important to note that in real world application the mass parameters of the cart and pendulum (barrel) may not always be exactly as expected. Our brief stated that there could be a variation in mass of up to 20%. This would have the most significant effect on the control system in the case of the pendulum being at its greatest possible mass and the cart at its lowest; reducing the overall system

controllability. However, when we tested our system against these extremes, we found that state-space still produced full rank controllability and observability matrices. Testing of both our original and looped LQR systems against this new state-space then showed that no system change would be required for successful control to be carried out. The only limitation of this is that, by the very nature of our state-space based control system, knowledge of the mass parameters is assumed. So, although the same systems could be used for carts and barrels of various masses, in a real world application it would be necessary to check these masses before running the control.

As for assumptions we made, such as the Stoke's Drag we used in the model, the limitation is clear that it can only be used under a low velocity of the cart[14]. If the cart exceeds a maximum velocity then the air flow changes from laminar to turbulent and our control system is likely to become unstable.

4.2 Further Advancements using Artificial Intelligence

Artificial intelligence can build on our robust system, adopting a different approach of learning and adapting to its oscillations. New algorithms are used on very complex problems, offering several possibilities creating a decision making situation for the controller [17]. This opens up the possibility of implementing this for our model once the automatic control has been simulated robustly. Integrating AI into our model would decrease the time for the system to stabilise to the equilibrium. Looking back to the upright human example, we could implement a reinforcement learning strategy where a controller uses trial-and-error methods to analyse the falling dynamics of a pendulum along with a reward function algorithm to make the controller learn. We can of course eliminate the human delay reaction time for our model, since we assume the barrels are loaded upright [7].

One method for artificial intelligence uses fuzzy logic, a many-valued logic form in which the truth values of variables may be continuous between 0 and 1 [18]. The fuzzy controller carries out a logical reduction process to stabilise the inverted pendulum in approx. 9.0s with a pendulum 4 times as big as the one we modelled, starting at an initial angle of 30°. Hence, having a faster stabilisation process due to the fuzzy controller. Whilst the input variables were different the graph shapes when stabilising were similar to our simulations [19]. Their robust testing simulation managed to start at 30° which is a more rigorous test compared to our maximum starting angle of 20°.

However, using further reinforcement learning can develop a controller for stabilization, which doesn't require input-output data, but it can get reward functions as feedback instead [20]. Under this condition, constraints of the angle can be reduced, leading to a wider range of rotation.

References

[1] EMILIO ROXIN. *Stability in General Control Systems* [online]. Available from: `https://www.sciencedirect.com/science/article/pii/002203966590015X#aep-bibliography-id4`, 1965–April(1). [Accessed 21 February 2020].

[2] Attila Becskei Luis Serrano. Engineering stability in gene networks by autoregulation [online]. Available from: `https://www.nature.com/articles/35014651.pdf`, 1 JUNE 2000. [Accessed 25 February 2020].

[3] Keith Pledger. Mechanics 4 [book], 10 Sep 2009. [Accessed 24 February 2020].

[4] Marvin Bugeja. Non-linear swing-up and stabilizing control of an inverted pendulum system. volume 2, pages 437 – 441 vol.2, 10 2003.

[5] S. K. Bhattacharya. *CONCEPT OF STABILITY* [online]. Available from: `https://www.oreilly.com/library/view/control-systems-engineering/9789332524392/`, 2013–May(1). [Accessed 21 February 2020].

[6] Raoul Herzog Jurg Keller. *An Overview on Robust Control* [online]. Available from: http://www.sga-asspa.ch/index_htm_files/2011-01%20an%20overview%20on%20robust%20control.pdf, 2011–September(19). [Accessed 24 February 2020].

[7] Ken Kiyono Yasushi Kobayashi Pietro Morasso Kenjiro Michimoto, Yasuyuki Suzuki and Taishin Nomura. *Reinforcement learning for stabilizing an inverted pendulum naturally leads to intermittent feedback control as in human quiet standing* [online]. Available from: https://www.ole.bris.ac.uk/bbcswebdav/pid-4170206-dt-content-rid-13609414_2/courses/EMAT22220_2019_TB-4/Michimoto2016.pdf, 2016–October(1). [Accessed 7 February 2020].

[8] Ioannis Kafetzis and Lazaros Moysis. Inverted pendulum: A system with innumerable applications. 03 2017.

[9] P. Labrot. *How does a seismometer work?* [online]. Available from: https://www.seis-insight.eu/en/public-2/planetary-seismology/how-a-seismometer-works, 7 November 2016. [Accessed 24 February 2020].

[10] JAN KOZÁK ANA CARNEIRO§ DAVID OLDROYD*, FILOMENA AMADOR** and MANUEL PINTO‡. *The Study of Earthquakes in the Hundred Years Following Lisbon Earthquake of 1755The Study of Earthquakes in the Hundred Years Following Lisbon Earthquake of 1755* [online]. Available from: https://www.researchgate.net/figure/Seismometer-designed-by-James-Forbes-1844-accompanying-plate_fig5_261697732, January 2007. [Accessed 24 February 2020].

[11] Navin John Mathew* K. Koteswara Rao* N. Sivakumaran***. Swing up and stabilization control of a rotary inverted pendulum [online]. Available from: https://www.sciencedirect.com/science/article/pii/S1474667015383324, December 18-20, 2013. [Accessed 25 February 2020].

[12] Joseph Peltroche and Anibal E. Morales Zambrana. Advanced mathematics for control system design [online]. Available from: https://ntrs.nasa.gov/archive/nasa/casi.ntrs.nasa.gov/20190002679.pdf, 04/11/2019. [Accessed 25 February 2020].

[13] MATLAB. *Inverted Pendulum: System Modelling* [online]. Available from: http://ctms.engin.umich.edu/CTMS/index.php?example=InvertedPendulum&section=SystemModeling, 2009. [Accessed 17 February 2020].

[14] Editors of Wikipedia. *Stokes's law* [online]. Available from: https://en.wikipedia.org/wiki/Stokes%27_law, 2011. [Accessed 27 February 2020].

[15] BISWA NATH DATTA. Controllability, observability, and distance to uncontrollability [online]. Available from: https://www.sciencedirect.com/topics/engineering/controllability-matrix, 2004. [Accessed 27 February 2020].

[16] Arthur Earl Bryson. *Applied optimal control: optimization, estimation and control.* Routledge, London, Jan 1975.

[17] T.Vámos. *Artificial Intelligence, Automatic Control and Development* [online]. Available from: https://www.sciencedirect.com/science/article/pii/S1474667017644070, 2017–June(28). [Accessed 24 February 2020].

[18] Editors of Wikipedia. Fuzzy logic [online]. Available from: https://en.wikipedia.org/wiki/Fuzzy_logic, 24 February 2020. [Accessed 27 February 2020].

[19] N. Yubazaki J. Yi*. Stabilization fuzzy control of inverted pendulum systems [online]. Available from: https://www.sciencedirect.com/science/article/pii/S0954181000000078, 15 March 2000. [Accessed 27 February 2020].

[20] Group 1032. Non-linear control and machine learning on an inverted pendulum on a cart [online]. Available from: https://projekter.aau.dk/projekter/files/281331409/Non_linear_Control_and_Machine_Learning_on_an_Inverted_Pendulum_on_a_Cart.pdf?fbclid=IwAR1tw2yt_r6FoF5FDaCF8pVUIna51o6-MUHbQp9qsjfusktUdvlD8lY__8E, 2018. [Accessed 27 February 2020].